Tutorials and Reviews

International Journal of Bifurcation and Chaos, Vol. 13, No. 2 (2003) 269–285

REVIEW OF CHAOS COMMUNICATION BY FEEDBACK CONTROL OF SYMBOLIC DYNAMICS

ERIK M. BOLLT*
Department of Mathematics and Computer Science,
Clarkson University, Potsdam, NY 13699-5815, USA
bolltem@clarkson.edu
http://www.clarkson.edu/∼bolltem

Received September 19, 2001; Revised November 30, 2001

This paper is meant to serve as a tutorial describing the link between symbolic dynamics as a description of a chaotic attractor, and how to use control of chaos to manipulate the corresponding symbolic dynamics to transmit an information bearing signal. We use the Lorenz attractor, in the form of the discrete successive maxima map of the z-variable time-series, as our main example. For the first time, here, we use this oscillator as a chaotic signal carrier. We review the many previously developed issues necessary to create a working control of symbol dynamics system. These include a brief review of the theory of symbol dynamics, and how they arise from the flow of a differential equation. We also discuss the role of the (symbol dynamics) generating partition, the difficulty of finding such partitions, which is an open problem for most dynamical systems, and a newly developed algorithm to find the generating partition which relies just on knowing a large set of periodic orbits. We also discuss the importance of using a generating partition in terms of considering the possibility of using some other arbitrary partition, with discussion of consequences both generally to characterizing the system, and also specifically to communicating on chaotic signal carriers. Also, of practical importance, we review the necessary feedback-control issues to force the flow of a chaotic differential equation to carry a desired message.

Keywords: Control of chaos; communication; communication with chaos; symbolic dynamics; hyperbolicity; synchronization; feedback control.

1. Introduction

The field of controlling chaos was first popularized by the simple "OGY" algorithm published in 1990 by Ott, Grebogi and Yorke [Ott *et al.*, 1990]. The idea is that an unstable periodic orbit can be stabilized by parametric feedback control once ergodicity has caused a randomly chosen initial condition to wander close enough to the periodicity that linear control theory can be applied [Ott *et al.*, 1990]. A tremendous flood of theoretical and experimental research has followed this seminal work, some of which extends the original OGY techniques, and some of which only has in common with OGY the simple realization that a chaotic oscillator is especially flexible and therefore allows for very sensitive selection between a wide range of possible behaviors.

Two major methods of communication with chaotic signal carriers are (1) Synchronization, and (2) Feedback control of symbolic dynamics. The subject of this paper concerns the feedback control symbolic dynamics approach, but we mention synchronization for contrast to the other school of

*More information can be found on the web: http://mathweb.mathsci.usna.edu/faculty/bolltem/

methods which are expected to appear here. The synchronization of chaotic oscillators phenomenon was first discovered in the early and mid-1980's by [Yamada & Fujisaka, 1983, 1984] and then [Afraimovich *et al.*, 1986], then in 1990 by [Pecora & Carroll, 1990] the last of which started an avalanche of research. Synchronization is now known to have fundamental implications in nature well beyond the practical engineering application of communication. To our interest here, it was shown very early on [Pecora & Carroll, 1990; Cuomo & Oppenheim, 1993] that using synchronization allows a chaotic signal carrier to transmit a message. See [Pecora *et al.*, 1997] for an excellent review. We also direct the reader to the very important practical engineering advances made by the European followers, as typified by the works [Kennedy & Kolumbán, 2000; Kolumbán & Kennedy, 2000; Kolumbán *et al.*, 1998] in noncoherent methods, including differential chaos shift keying (DCSK) modulation schemes.

On the other hand, control of symbolic dynamics relies on a fundamental description of a chaotic oscillator by change of coordinates that brings a discrete time map (which may arise by a flow mapping between Poincaré surfaces) on its phase space to an abstract Bernoulli shift map on some subshift space. The fundamental link between chaotic oscillators and symbolic dynamics was first introduced by Smale [1967]. In 1993, Hayes *et al.* [1993, 1994] showed that feedback control of chaotic trajectories together with sensitive dependence and the symbolic dynamical description of chaotic trajectories can be used to force a chaotic oscillator to carry information. Small parametric feedback control sensitively alters a chaotic trajectory and hence said change of coordinates serves as a coding function to transform the symbolic sequence corresponding to the original chaotic trajectory, into some other symbolic sequence corresponding to a desired message. We would also like to point out to the reader that at time of press, a closely related article on communication in chaos using symbol dynamics has appeared [Schweizer & Schimming, 2001a, 2001b].

While this paper is meant to serve as a tutorial, as our main example, we will show for the first time how Lorenz's successive maxima map serves as a good information carrying device. In our previous work the author and Dolnik [Bollt & Dolnik, 1997; Dolnik & Bollt, 1998] considered a chemical system. Since it has been shown that the Lorenz equations can be easily realized in circuitry [Cuomo & Oppenheim, 1993], it follows that such a system could in principle be built. In Sec. 2, we review the Lorenz system and attractor, which will serve as our main concrete example, and we discuss how the successive maxima map yields a one-humped map, for which the symbol dynamics are defined. We review in Sec. 3 the necessary symbolic dynamics, both for general diffeomorphisms of the plane, and for the simpler chaos of one-dimensional many-to-one maps, of which the successive maxima map of the Lorenz flow is an example. Then in Sec. 4, we discuss both the role and importance of using a generating partition. We also discuss the consequences of using a nongenerating (arbitrary) partition, both in describing the system, and also specifying the consequences to communicating with chaos. We briefly review a new algorithm to use collections of unstable periodic orbits to reveal the generating partition. In Sec. 5, we recall a technique, codeveloped by the author [Bollt *et al.*, 1997; Bollt & Lai, 1998; Lai & Bollt, 1999], whereby a great deal of channel noise resistance can be added to the system, and costs only a minor loss of transmitter capacity, simply by restricting trajectories to always avoid a neighborhood of the generating partition. Our feedback control techniques discussed in Sec. 6 will follow the methods codeveloped by the author in [Dolnik & Bollt, 1998], in which we allow for all necessary information to be learned purely by observation and measurement, in the setting of a laboratory experiment, and in the absence of a closed form differential equation model of the dynamical system.

2. Lorenz Differential Equations and Successive Maxima Map

We consider the Lorenz system [Lorentz, 1963],

$$\begin{aligned} \dot{x} &= 10(y - x)\,, \\ \dot{y} &= x(28 - z) - y\,, \\ \dot{z} &= xy - \frac{8}{3}z\,, \end{aligned} \tag{1}$$

both because it is a benchmark example of chaotic oscillations, and because it can be physically realized by an electronic circuit [Cuomo & Oppenheim, 1993]. Likewise those interested in optical transmission carriers may recall the Lorenz-like infrared NH3 laser data [Huebner *et al.*, 1989]. E. Lorenz showed that his equations have the property that the successive local maxima can be described by a

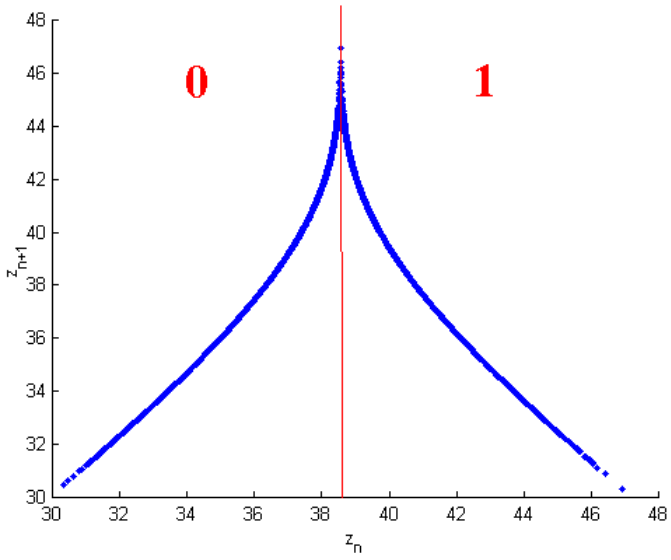

Fig. 1. Successive maxima map of the measure $z(t)$ variable, of the Lorenz flow $(x(t), y(t), z(t))$ from Eqs. (1).

one-dimensional, one-hump map,

$$z_{n+1} = f(z_n)\,, \tag{2}$$

where we let z_n be the nth local maximum of the state variable $z(t)$. The chaotic attractor in the phase space $(x(t), y(t), z(t))$ shown in Fig. 1 corresponds to a one-dimensional chaotic attractor in the phase space of the discrete map $f(z)$, and hence the symbol dynamics are particularly simple to analyze. See Fig. 2. The generating partition for defining a good symbolic dynamics is the critical point z_c of the $f(z)$ function. A trajectory point with

$$z < z_c (z > z_c) \text{ bears the symbol } \mathbf{0}\ (\mathbf{1})\,. \tag{3}$$

The partition of this one-dimensional map, of successive $z(t)$ maxima corresponds to a traditional Poincaré surface mapping, as the two leaves of the surface of section can be seen in Fig. 1. Each bit roughly corresponds to a rotation of the $(x(t), y(t), z(t))$ flow around the left or the right lobes of the Lorenz butterfly-shaped attractor. However, the Lorenz attractor does not allow arbitrary permutations of rotations around one and then the other lobe; the corresponding symbolic dynamics has a somewhat restricted grammar which must be learned. The grammar of the corresponding symbolic dynamics completely characterizes the allowed trajectories. Since the purpose of this paper is to show how a chaotic oscillator can be forced to carry a message in its symbolic dynamics, we develop further these notions in the next section.

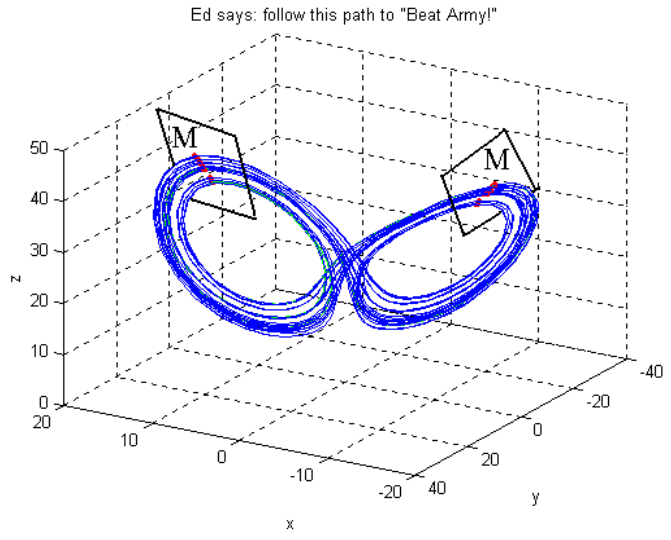

Fig. 2. Lorenz's butterfly attractor. This particular "typical" trajectory of Eqs. (1) gives the message "Beat Army!" when interpreted relative to the generating partition Eq. (3) of the one-dimensional successive maxima map Eq. (2) shown in Fig. 2.

3. Symbolic Dynamics

In this section, we review the mathematical change of coordinates which allows trajectories of a discrete dynamical system to be equivalently described as infinite bit streams. Such symbolic dynamical descriptions of chaos were first invented as a simplifying change of coordinates, in which the proofs of many theorems become simple [Robinson, 1995]. Indeed, most of the dynamical systems for which mathematically rigorous proof exists concerning their chaotic properties are precisely those for which a conjugacy to some symbolic shift exists (see examples in [Robinson, 1995; Devaney, 1989]. For our purposes in communications describing controlled trajectories as messages involve conversion to a bit stream as a crucial step.

3.1. *One-dimensional maps with a single critical point*

First we consider a one-humped interval map, such as the situation of Lorenz's successive maxima map.

$$f : [a, b] \to [a, b]\,. \tag{4}$$

Such a map "has" symbolic dynamics [Milnor & Thurston, 1977; de Melo & van Strein, 1992] relative to a partition at the critical point x_c. Choose

a two symbol partition, labeled $\mathcal{I} = \{0, 1\}$, naming iterates of an initial condition x_0 according to,

$$\sigma_i(x_0) = \begin{pmatrix} 0 & \text{if } f^i(x_0) < x_c \\ 1 & \text{if } f^i(x_0) > x_c \end{pmatrix} . \quad (5)$$

The function h which labels each initial condition x_0 and corresponding orbit $\{x_0, x_1, x_2, \ldots\}$ by an infinite symbol sequence is,

$$h(x_0) \equiv \sigma(x_0) = \sigma_0(x_0) \cdot \sigma_1(x_0)\sigma_2(x_0) \ldots . \quad (6)$$

Defining the "fullshift" $\Sigma_2 = \{\sigma = \sigma_0 \cdot \sigma_1\sigma_2 \ldots$ where $\sigma_0 = 0$ or $1\}$ to be the set of all possible infinite symbolic strings of 0's and 1's, then any given infinite symbolic sequence is a singleton (a point) in the fullshift space, $\sigma(x_0) \in \Sigma_2$. The usual topology of open sets in the shift space Σ_2 follows the metric,

$$d_{\Sigma_2}(\sigma, \overline{\sigma}) = \sum_{i=0}^{\infty} \frac{|\sigma_i - \overline{\sigma}_i|}{2^i} , \quad (7)$$

which defines two symbol sequences to be close if they agree in the first several bits. Equation (5) is a good "change of coordinates," or more precisely a homeomorphism,[1]

$$h : [a, b] - \bigcup_{i=0}^{\infty} f^{-i}(x_c) \to \Sigma_2' , \quad (8)$$

under conditions on f, such as piecewise $|f'| > 1$.[2] The Bernoulli shift map moves the decimal point in Eq. (6) to the right, and "eliminates" the leading symbol,

$$s(\sigma_i) = \sigma_{i+1} . \quad (9)$$

All of those itineraries from the map f, Eq. (4) by Eq. (5), correspond to the Bernoulli shift map restricted to a subshift,[3] $s : \Sigma_2' \to \Sigma_2'$. Furthermore, the change of coordinates h respects the action of the map, it commutes, and it is a conjugacy.[4]

In summary, the previous paragraph simply says that corresponding to the orbit of each initial condition of the map Eq. (4), there is an infinite itinerary of 0's and 1's, describing each iterate's position relative to the partition in a natural way which acts like a change of coordinates such that the dynamical description is equivalent. For our purposes, controlling orbits of the map f in phase space which is an interval corresponds also to controlling itineraries in symbol space. The control over x composed with the change of coordinates h can essentially be considered to be a coding algorithm.

3.2. *Learning the grammar in practice*

In a physical experiment, corresponding to the one-dimensional map such as Eq. (4), it is possible to approximately deduce the grammar of the corresponding symbolic dynamics by systematic recording of the measured variables. First note that any real measurement of an experiment consists of a necessarily finite data set. Therefore, in practice, it can be argued that there is no such thing as a grammar of infinite type in the laboratory.[5] So without loss of generality, we may consider only grammars of finite type for our purposes. Such a subshift is a special case of a sophic shift [Kitchens, 1998; Lind & Marcus, 1995]. In other words, there exists a finite digraph which completely describes the grammar. All allowed words of the subshift, Σ' corresponding to itineraries of orbits of the map correspond to some walk through the graph.

For example, the full 2-shift shift is generated by the graph in Fig. 3(a) (but this is not the minimal graph generating Σ_2). Likewise, the "No two zero's in a row" subshift Σ_2' is generated by all possible infinite walks through the digraph in

[1]A *homeomorphism* between two topological spaces A and B is a one-one and onto continuous function $h : A \to B$, which may be described loosely as topological equivalence.

[2]Note that preimages of the critical point are removed from $[a, b]$ for the homeomorphism. This leaves a Cantor subset of the interval $[a, b]$. This is necessary since a shift space is also closed and perfect, whereas the real line is a continuum. This is an often overlooked technicality, which is actually similar to the well known problem when constructing the real line in the decimal system (the ten-shift Σ_{10}) which requires identifying repeating decimal expansions of repeating 9's such as for example $1/5 = 0.1\overline{99} \equiv 0.2$. The corresponding operation to the shift maps [Devaney, 1989] is to identify the repeating binary expressions $\sigma_0 \cdot \sigma_1 \cdots \sigma_n 0\overline{11} \equiv \sigma_0 \cdot \sigma_1 \cdots \sigma_n 1\overline{11}$, thus "closing the holes" of the shift space Cantor set.

[3]A *subshift* Σ_2' is a closed and Bernoulli shift map invariant subset of the fullshift, $\Sigma_2' \subset \Sigma_2$.

[4]A *conjugacy* is a homeomorphism h between topological spaces A and B, which commutes maps on those two spaces, $\alpha : A \to A$, $\beta : B \to B$, then $h \circ \alpha = \beta \circ h$.

[5]It could be furthermore argued that there is no such thing as measuring chaos in the laboratory, since the most popular definitions of chaos [Devaney, 1989] are asymptotic requiring sensitive dependance and topological transitivity, both of which would require time going to infinity to confirm.

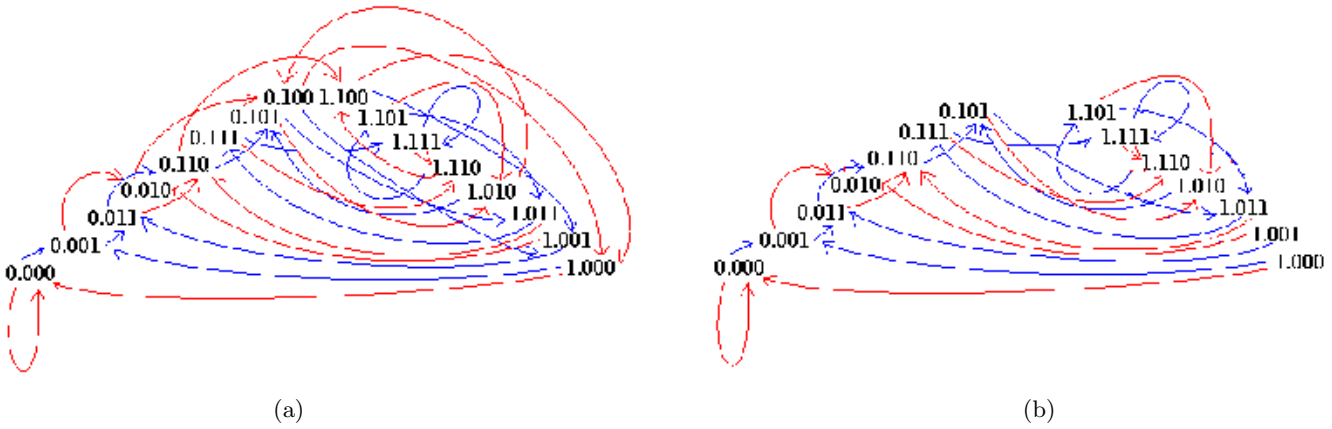

(a) (b)

Fig. 3. The full 2-shift Σ_2 is generated by all possible infinite walks through (a) above digraph. (b) The "No two zero's in a row" subshift grammar Σ_2' is generated by all possible infinite walks through the above digraph, in which the only two vertices corresponding to "00" words have been eliminated, together with their input and output edges. Blue denotes transitions which shift a "1" into the bit-register, and red denotes a "0" shift.

Fig. 3(b), in which the only two vertices corresponding to "00" words have been eliminated, together with their input and output edges. Given a finite measured data set $\{x_i\}_{i=0}^N$, simply by recording all *observed* words of length n corresponding to observed orbits, and recording this list amongst all possible 2^n such words, the appropriate digraph can be constructed as in Fig. 3. One should choose n to be the length of the observed minimal forbidden word. Sometimes, n is easy to deduce by inspection as would be the case if it were "00" as in Fig. 3(b), but difficult to deduce for larger n. There exist more systematic algorithms to deduce the minimal forbidden word length, such as the subgroup construction developed in [Bollt *et al.*, 2000; Bollt *et al.*, 2001] related to the "follower-set" construction [Kitchens, 1998; Lind & Marcus, 1995].

Since, the data set $\{x_i\}_{i=0}^N$ is finite, then if the true minimal forbidden word corresponding to the dynamical system is longer than data sample size, $n > N$, only an approximation of the grammar is possible. Therefore the corresponding observed subshift is expected to be a subset of whatever might be the true subshift of the model map Eq. (4) or experiment. This is generally not a serious problem for our purposes since some course-graining always results in an experiment, and this sort of error will be small as long as the word length is chosen to be reasonably large without any observed inconsistencies. Typically, we assume that $N \gg n$. As a technical note of practical importance, we have found link-lists to be the most efficient method to record a directed graph together with its allowed transitions.

In Sec. 5, we discuss how the grammar can be deliberately restricted to offer improved channel noise resistance.

3.3. *One-dimensional maps with several critical points*

In general, an interval map Eq. (4) may have n critical points $x_{c,j}$, $j = 1, 2, \ldots, n$, and hence there may be points $x \in [a, b]$ with up to $n + 1$-preimages. Therefore, the symbol dynamics is naturally generalized [Lind & Marcus, 1995] by expanding the symbol set $\mathcal{I} = \{0, 1, \ldots, n\}$ to define the shift space Σ_{n+1}. The subshift $\Sigma'_{n+1} \subset \Sigma_{n+1}$ of itineraries corresponding to orbits of the map Eq. (4) follows the obvious generalization of Eq. (5), $\sigma_i(x_0) = j$ if $x_{c,j} < f^i(x_0) < x_{c,j+1}$, $j = 0, 1, \ldots, n + 1$, and taking $x_{c,0} = a$ and $x_{c,n+1} = b$. The characterization of the grammar of the resulting subshift Σ'_{n+1} corresponding to a map with n-turning points is well developed following the kneading theory of Milnor and Thurston [1977]. See also [de Melo & van Strein, 1992].

3.4. *More than one dimension and symbolic dynamics of diffeomorphisms*

Diffeomorphisms arise naturally by Poincaré mapping of a flow. In general, a diffeomorphism $f\colon M \to M$ is expected for an $N - 1$ manifold M which is transverse to a flow in $\mathbf{R}^N$.

Symbolic dynamics of higher dimensional systems is still a highly active research area and details

here are necessarily slight. In particular, we refer the reader to see [Cvitanovic, 1988, 1991, 1995]. The fundamental difference of dimensionality is that invertible maps and hence diffeomorphisms are necessarily simple in the interval, whereas in more than one dimension, there may be chaos. In the interval, only a many-to-one map allows for the folding property which is an ingredient of chaos. However, Smale [1967] showed that the folding mechanism of a horseshoe allows for chaos in a planar diffeomorphism.

In the development in the previous subsections, the one-sided shifts reflect the noninvertible nature of the corresponding interval maps Eq. (4). The generalization of symbolic dynamics for invertible maps requires bi-infinite symbol sequences,

$$\Sigma_2 = \{\sigma = \cdots \sigma_{-2}\sigma_{-1}\sigma_0 \cdot \sigma_1\sigma_2 \ldots \quad \text{where } \sigma_0 = 0 \text{ or } 1\}\,. \tag{10}$$

The main technical difficulty of symbolic dynamics for a map with a more than one-dimensional domain is to well define a partition. A notion of Markov partitions is well defined[6] for Axiom A diffeomorphisms [Bowen, 1975a], but such maps are not expected to be generic. The more general notion of a generating partition [Rudolph, 1990] is also well defined,[7] but particularly in the case of a nonuniformly hyperbolic dynamical system construction of the generating partition is an open problem for most maps. A well regarded conjecture for planar diffeomorphisms, such as the Hénon map [Cvitanovic *et al.*, 1988; Cvitanovic, 1991], is that the generating partition should be a curve that connects all "primary" homoclinic tangencies. See also [Grassberger *et al.*, 1989; Christiansen & Politi, 1996, 1997; Hansen, 1992, 1993].

A main feature in the definition of a generating partition is that symbolic itineraries uniquely define trajectories of the map.

4. The Role of the Partition

At the end of the previous section, we mentioned the difficulty in finding a generating partition of the symbolic dynamics for dynamical systems in more than one dimension in practice, and in particular, in the sorts of dynamical systems which might arise from a physical application. In this section, we mention two ways to address this fundamental obstacle to controlling symbolic dynamics.

4.1. *Is a generating partition really necessary?*

In [Bollt *et al.*, 2000, 2001] we studied in rigorous mathematical detail the consequences of using an arbitrarily chosen partition, which is generally not generating. Our previous work cited was motivated by the many recent experimentalists' studies, who with measured time-series data in hand, but in the absence of a theory leading to a known generating partition, simply choose a threshold crossing value of the time-series to serve as a partition of the phase space.

On the experimental side, there appears an increasing interest in chaotic symbolic dynamics [Kurths *et al.*, 1995; Lehrman & Rechester, 1997; Daw *et al.*, 1998; Engbert *et al.*, 1998; Mischaikow *et al.*, 1999]. A common practice is to apply the threshold-crossing method, i.e. to define a rather arbitrary partition, so that distinct symbols can be defined from measured time series. There are two reasons for the popularity of the threshold-crossing method: (1) it is extremely difficult to locate the generating partition from chaotic data, and (2) threshold-crossing is a physically intuitive and natural idea. Consider, for instance, a time series of temperature $T(t)$ recorded from a turbulent flow. By replacing the real-valued data with symbolic data relative to some threshold T_c, say a **0** if $T(t) < T_c$ and a **1** if $T(t) > T_c$, the problem

[6]Bowen [1970, 1975b], defined conditions for a partition of "rectangles" to be Markov. A topological partition $\{Q_i\}$ of open rectangles is Markov if, $\{Q_i\}$ have nonoverlapping interiors, such that when $f(Q_i) \cap Q_j \neq \emptyset$, then $f(Q_i)$ stretches across Q_j, in that stretching directions are mapped to stretching directions and contracting directions are mapped to contracting directions. Said more carefully, we require that $W^u(f_n(z), Q_i) \subset f_n(W^u(z, Q_i)$ and $f_n(W^s(z, Q_i) \subset W^s(f_n(z), Q_i)$.

[7]Given a dynamical system $f : M \to M$, a *finite* collection of disjoint open sets, $\{B_k\}_{k=1}^K$, $B_k \cap B_j = \emptyset$ $(k \neq j)$, is defined to be a topological partition if the union of their closures exactly covers $M : M = \cup_{k=1}^K \overline{B}_k$, [Lind & Marcus, 1995]. The set of intersection of the images and preimages of these elements $\cap_{i=-n}^{n} \mathbf{f}^{(-i)}(B_{\mathbf{x}_i})$ is in general open. For a faithful symbolic representation of the dynamics, the limit $\cap_{n=0}^{\infty} \cap_{i=-n}^{n} \mathbf{f}^{(-i)}(B_{\mathbf{x}_i})$ should be a single point if nonempty. Given a dynamical system $\mathbf{f} : \mathcal{M} \to \mathcal{M}$ on a measure space $(\mathcal{M}, F, \mu)$, a finite partition $P = \{B_k\}_{k=1}^K$ is generating if the union of all images and preimages of P gives the set of all μ-measurable sets F. In other words, the "natural" tree of partitions: $\vee_{i=-\infty}^{\infty} \mathbf{f}^i(P)$, always generates some sub-σ-algebra, but if it gives the full σ-algebra of all measurable sets F, then P is called *generating* [Rudolph, 1990].

of data analysis can be simplified. A well chosen partition is clearly important: for instance, T_c cannot be outside the range of $T(t)$ because, otherwise, the symbolic sequence will be trivial and carry no information about the underlying dynamics. It is thus of paramount interest, from both the theoretical and experimental points of view, to understand how misplaced partitions affect the goodness of the symbolic dynamics such as the amount of information that can be extracted from the data.

As a model problem, we chose to analyze the tent map

$$f : [0,\,1] \to [0,\,1],\;\; x \to 1 - 2|x - 1/2|\,, \qquad (11)$$

for which most of our proofs can be applied. Our numerical experiments indicated that the results were indicative of a much wider class of dynamical systems, including the Hénon map, and experimental data from a chemical reaction.

The tent map is a one-humped map, and it is known that the symbolic dynamics indicated by the generating partition at $x_c = 1/2$, by Eq. (5) gives the full 2-shift Σ_2, on symbols $\{0,\,1\}$. The topological entropy of $\Sigma_2^{\{\mathbf{0},\mathbf{1}\}}$ is ln 2. Now misplace the partition at

$$p = x_c + d\,, \quad \text{where } d \in \left[-\frac{1}{2},\,\frac{1}{2}\right]\,, \qquad (12)$$

is the misplacement parameter. In this case, the symbolic sequence corresponding to a point $x \in [0,\,1]$ becomes:

$$\begin{aligned} &\phi = \phi_0 \cdot \phi_1\phi_2 \ldots\,, \\ \text{where} \quad &\phi_i(x) = \mathbf{a}(\mathbf{b}) \text{ if } f^i(x) < p(> p)\,, \end{aligned} \qquad (13)$$

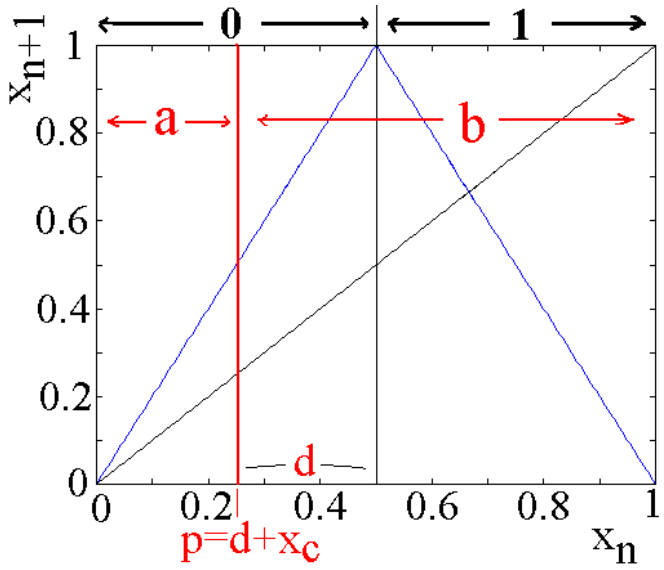

Fig. 4. Tent map and a misplaced partition at $x = p$.

as shown in Fig. 4. The shift so obtained: $\Sigma_2^{\{\mathbf{a},\mathbf{b}\}}$, will no longer be a full shift because not every binary symbolic sequence is possible. Thus, $\Sigma_2^{\{\mathbf{a},\mathbf{b}\}}$ will be a subshift on two symbols **a** and **b** when $d \neq 0$ ($p \neq x_c$). The topological entropy of the subshift $\Sigma_2^{\{\mathbf{a},\mathbf{b}\}}$, denoted by $h_T(d)$, will typically be less than $h_T(0) = \ln 2$. Numerically, $h_T(d)$ can be computed by using the formula [Robinson, 1995]:

$$h_T(d) = \lim_{n\to\infty} \sup \frac{\ln N_n}{n}\,, \qquad (14)$$

where $N_n \leq 2^n$ is the number of (**a**, **b**) binary sequences (words) of length n. In our computation, we choose 1024 values of d uniformly in the interval $[-1/2,\,1/2]$. For each value of d, we count N_n

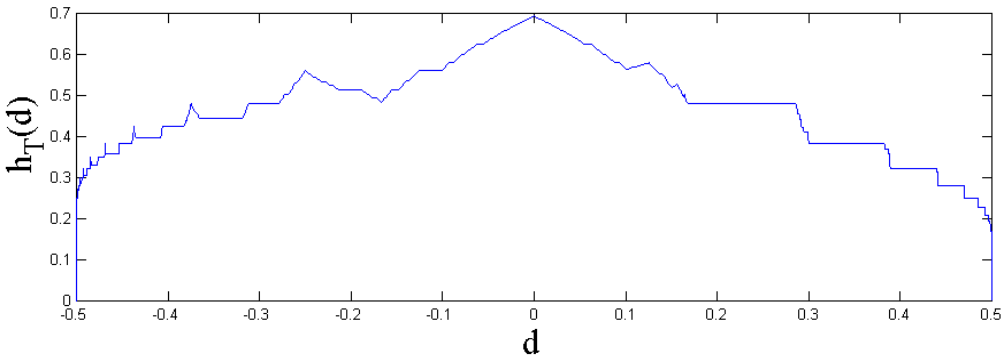

Fig. 5. For the tent map: Numerically computed $h_T(d)$ function by following sequences of a chaotic orbit.

in the range $4 \leq n \leq 18$ from a trajectory of 2^{20} points generated by the tent map. The slopes of the plots of ln N_n versus n approximates to h_T. Figure 5 shows $h_T(d)$ versus d for the tent map, where we observe a complicated, devil's staircase-like, but clearly nonmonotone behavior. For $d = 0$, we have $h_T(0) \approx \ln 2$, as expected. For $d = -1/2$ $(1/2)$, from Fig. 4, we see that the grammar forbids the letter **a** (**b**) and, hence, $\Sigma_2^{\{\mathbf{a},\mathbf{b}\}}(-1/2)[\Sigma_2^{\{\mathbf{a},\mathbf{b}\}}(1/2)]$ has only one sequence: $\phi = \mathbf{b} \cdot \mathbf{b}\overline{\mathbf{b}}$ $(\phi = \mathbf{a} \cdot \mathbf{a}\overline{\mathbf{a}})$. Hence, $h_T(\pm 1/2) = 0$.

Many of our techniques were somewhat combinatorial, relying on a simple idea that a dense set of misplacement values (in particular if d is "dyadic", of the form $d = p/2^n$), allows us to study the related problem of counting distinctly colored paths through an appropriate graphic presentation of the shift, in which vertices have been relabeled according to where the misplacement occurs. See Fig. 6.

One of our principal results was a rigorous proof that the entropy can be a nonmonotone and devil's staircase-like function of the misplacement parameter. As such, the consequence of a misplaced partition can be severe, including significantly reduced topological entropies and a high degree of nonuniqueness. Of importance to the experimentalist who wishes to characterize a dynamical system by observation of a bit stream generated from the measured time-series, we showed that interpreting

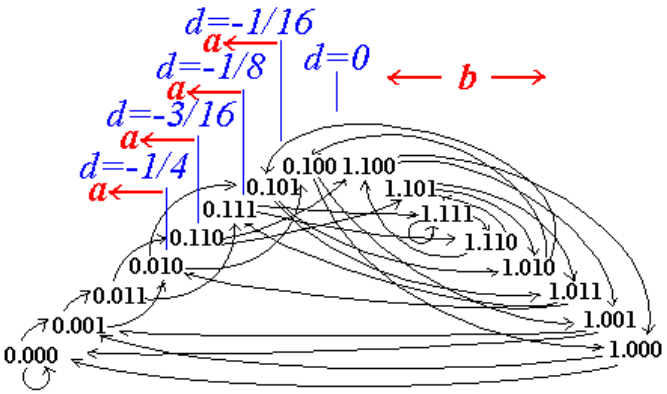

Fig. 6. Graphic presentation for the Bernoulli fullshift and some dyadic misplacements. Placing the partion at $p = (1/2) + d$, $-(1/2) \leq d \leq 1/2$, and d as dyadic, such as $d = 0$, $-1/16$, $-1/8$, $-3/16$, or, $-1/4$, as shown, corresponds to a relabeling of the originally right resolving presentation of the fullshift. The 16 4-bit words are arranged above monotonically with the kneading order of a one-hump map, and so the relabeling occurs in a predictable fashion: shifts to a on the left, and to b on the right, and the details of the relabeling depends on the chosen values of d, some of which are shown.

any results obtained from threshold-crossing type of analysis should be exercised with extreme caution. While apparently by computer experiment, entropy is continuous with partition placement, an arbitrarily chosen partition is expected not to be close to the true partition, and also there can be severe nonuniqueness problems.

Specifically, we proved that the splitting properties of a generating partition are lost in a severe way. We defined a point x to be p-undistinguished if there exists a point $y \neq x$ such that the p-named $a - b$ word according to Eq. (13) does not distinguish the points, $\phi(x) = \phi(y)$. We defined a point x to be uncountably p-undistinguished, if there exists uncountable many such y. We proved a theorem in [Bollt *et al.*, 2001] that states that if $p = q/2^n \neq 1/2$, then the set of uncountably p-undistinguished initial conditions is dense in $[0, 1]$. In other words, the inability of symbolic dynamics from the "bad" nongenerating partition to distinguish the dynamics of points is severe. We described the situation as being similar to that of trying to interpret the dynamical system by watching a projection of the true dynamical system. In this scenario, some "shadow", or projection of the points correspond to uncountably many suspension points. In our studies [Bollt *et al.*, 2000; Bollt *et al.*, 2001] we also gave many further results both describing the mechanism behind the indistinguishability, and further elucidating the problem.

Now we return to the problem of communicating with chaos. Is it possible to transmit a message on a chaotic carrier despite using other than the generating partition? In Eqs. (5) and (6) we describe the function, $\sigma : [0, 1] \to \Sigma_2^{\{\mathbf{0},\mathbf{1}\}}$ and in Eq. (13), the function $\phi : [0, 1] \to \Sigma_2^{\{\mathbf{a},\mathbf{b}\}}$. Hence, we imply a function $p : \Sigma_2^{\{\mathbf{0},\mathbf{1}\}} \to \Sigma_2^{\{\mathbf{a},\mathbf{b}\}}$ which is uncountably-many-to-one at some points. Nonetheless, each initial condition $x \in [0, 1]$ has an $a - b$ sequence, and if we know how to control arbitrarily (the $0 - 1$ corresponding sequence) the orbit of x by feedback control, we are correspondingly controlling its $a - b$ sequence. While each x has one corresponding code-image $\phi(x)$, since ϕ is a well defined function, it is not necessarily a problem for the purpose of communication that $\phi(x)$ can be uncountably-many-to-one. So in the situation that the transmitter plant knows the dynamical system very well, meaning how to control trajectories arbitrarily (knowing how to control its true underlying $\Sigma_2^{\{\mathbf{0},\mathbf{1}\}}$ symbolic dynamics) *to infinite precision* then

the transmitter is also controlling the corresponding $\Sigma_2^{\{\mathbf{a},\mathbf{b}\}}$ symbol dynamics. The receiver need only know the key, which requires knowing the partition p in Eq. (13). If on the other hand, the transmitter does not know the underlying generating partition, then the poor continuity properties of the ϕ function make the situation impractical, to say the least. Of course, the assumption of infinite precision is ridiculous for an experiment. It turns out that if a small channel error occurs, then the received bit will be misinterpreted — meaning a received error can occur. The solution for the generating partition discussed in Sec. 5 is also much more difficult when not using the generating partition. A final consequence of trying to use a nongenerating partition would be reduced topological entropy, and hence reduced transmitter capacity, which is an issue also further discussed in Sec. 5.

In fact, a recent application in chaotic cryptography makes use of "misplacing" the partition *deliberately* as a cryptic key [Alvarez *et al.*, 1999].

4.2. *The skeleton of periodic orbits and generating partitions*

Davidchack *et al.* [Ruslan *et al.*, 2000] have recently shown that symbolic dynamics can be learned solely by observation of a large collection of the unstable periodic orbits of the dynamical system. It has been said by Cvitanovic [1988, 1991, 1995] that periodic orbits are the "skeleton" of chaos, meaning that the complete collection of periodic orbits reveals the ergodic properties of a dynamical system.

There are several recent advancements both in computer hardware, and general algorithms [Davidchack *et al.*, 1999; Schmelcher & Diakonos, 1998, 1997; Diakonos *et al.*, 1998] that make it reasonable to collect the hundreds of thousands of periodic orbits of periods up to say 25 to 30 for well known maps such as Hénon or Ikeda, with a certain amount of confidence that *all* have been collected. Interval Newton's method and bisection method can be used to guarantee that no periodic orbits are missed, say for Hénon map successfully for periods up to 30 [Galais, 1999, 2001, 2002]. Since the definition of a generating partition requires that every initial condition be named uniquely by the symbol dynamics, in particular, a well defined partition must label each of these numerically collected periodic orbits uniquely. This is the concept of splitting which is necessary to well define a generating partition. In [Ruslan *et al.*, 2000], we devised a so-called "proximity" function to create a simple algorithm whereby the "complete" list of collected orbits could be checked against a proposed trial partition, which is then refined in a systematic and decreasing way relative to the proximity function which moves the partition as little as possible on each trial. By creating partitions which are consistent for all periodic orbits through period-m, say, then on each refinement to the next order period, $m+1$, we find that the corrections to the partition position become increasingly small. In particular, see [Ruslan *et al.*, 2000] for a color picture of the Ikeda map partition, first found by this method. Perhaps the most interesting feature of this technique, is that once lists of periodic orbits have been collected, the technique is essentially dimension independent, since one is simply "painting" and then "repainting" lists of numbers in a specified order. The interested reader should investigate an alternative algorithm by [Lefranc *et al.*, 1994; Boulant *et al.*, 1997a, 1997b] to find the generating partition, also by using periodic orbits, but by methods which are theoretically deeply rooted in the theory of templates and the knotted structure of periodic orbits of flows in three dimensions.

5. Dealing with Noise by Code Restrictions

It is no surprise that channel noise can disrupt a signal transmission, but unchecked, controlled symbolic dynamics would be particularly suseptible to bit errors even with small amplitude channel noise. It turns out that there is a very simple way to greatly reduce the vulnerability of a transmitted signal to misinterpretation due to channel noise, by a technique developed by the author and colleagues [Bollt *et al.*, 1997; Bollt & Lai, 1998; Lai & Bollt, 1999].

If the measured variable x is targeted to a point near the generating partition at x_c, then a small noise amplitude in this measurement can frequently cause the opposite bit than the intended transmission to be interpreted by the receiver. For example, in Fig. 2, if $z(t)$ is controlled to just to the left of the partition line, at approximately $z_c \approx 38.5754$, then even a small noise amplitude may cause that measurement to be misinterpreted as being to the right of the partition. In addition to the below described scheme, one could use an error correcting code, such as the Viterbi algorithm [Forney,

1975; Heller & Jacobs, 1971; Lin & Costello, 1982; Michelson & Levesque, 1985; Peterson & Weldon, 1998; Pless, 1998] in the case of Gaussian noise to further improve noise resistance, rather than transmitting plain ascii with the symbol masking as we have described below for clarity.

5.1. *Introducing a code restriction — Communicating on unstable chaotic saddles*

The solution to avoid channel noise is simple: avoid targeting a neighborhood of the partition. Suppose x_0 is targeted to $x_1 = x_c + \varepsilon$ to input, say, a "1"-bit into the bit register, then a channel noise of amplitude ε can push x_1 below x_c, and the receiver interprets a "0"-bit. Simply, never targeting a gap $(x_c - \varepsilon,\ x_c + \varepsilon)$ prevents this problem. But then in dynamical systems, it is not possible to simply remove a region from the phase space; it is necessary to dynamically remove the region by removing it and all of its preimages. The remaining set,

$$M(\varepsilon) = [0,\ 1] - \cup_{i=0}^{\infty} f^{-i}((x_c - \varepsilon,\ x_c + \varepsilon))\,, \quad \varepsilon > 0\,, \tag{15}$$

leaves a Cantor set, which for many one-humped maps, including that in Fig. 2, is nonempty for small enough ε. See Fig. 7. Such invariant sets are called unstable chaotic saddles embedded in the full interval invariant set. We have found that they are highly useful for communicating with chaos, since they are noise resistant, easy to stabilize, and cost only a relatively small amount of transmitter capacity, as we discuss below. Also important, is the fact that these sets can be characterized as a subshift embedded in the subshift of the full interval, and hence they can be specified by a simple code restriction.

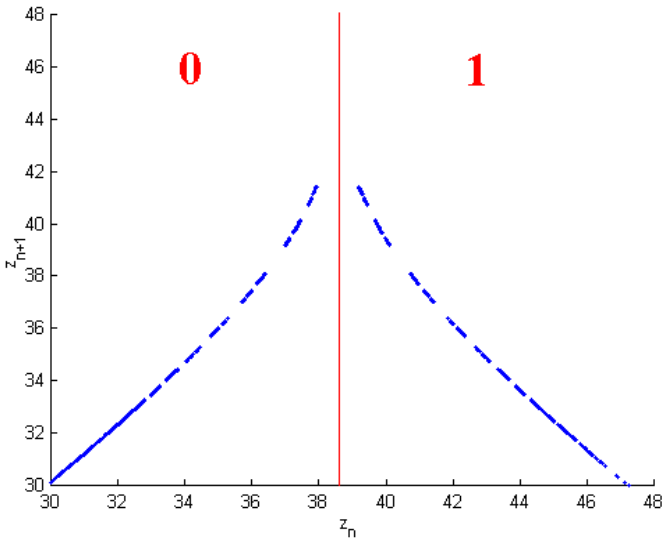

Fig. 7. An unstable chaotic saddle $M(s)$ remains after a gap is removed around the generating partition, as per Eq. (15). This Cantor set has favorable channel noise resistance properties as a message carrier, but costs to the transmitter capacity is only slight, as shown in Fig. 8.

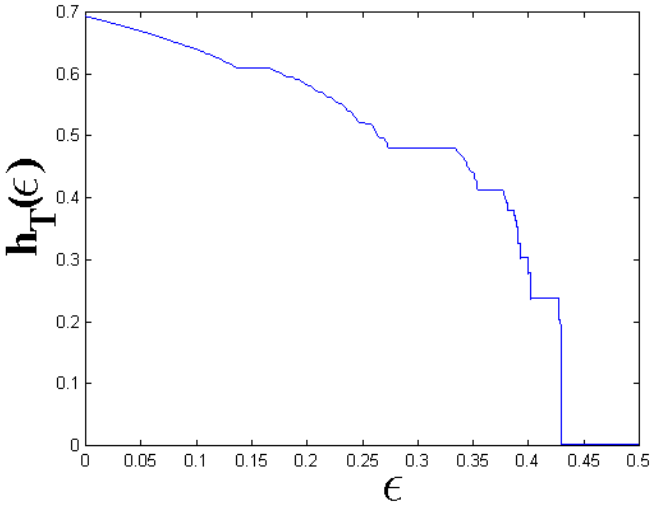

Fig. 8. Topological entropy $h_T(\varepsilon)$ as a function of noise gap ε. At each fixed value of ε, the topological entropy of the unstable chaotic saddles $M(\varepsilon)$ in Eq. (15) are shown, one of which is depicted in Fig. 7. Notice that initially, even a fairly large noise gap ε costs only a modest decrease in $h_T(\varepsilon)$, relative to maximal at $\varepsilon = 0$.

A simple fact from the kneading theory [Milnor & Thurston, 1977] provides that the codes of the unit interval are ordered monotonically in the unit interval when choosing the "Gray-Code" order $\prec$. That is $x < y$ implies $\sigma(x) \preceq \sigma(y)$. In Fig. 3(a), the 4-bit words are arranged left to right according to "$\prec$". Therefore, an ε-neighborhood of x_c can be characterized by a range of codes, and approximated by some n-bit code restriction. For example, the Lorenz map allows the 4-bit words 0.100 and 1.100, which can be seen in Fig. 3(a), and defines an ε-neighborhood of x_c, $(x_c - \varepsilon,\ x_c + \varepsilon)$. To avoid this neighborhood, it is necessary to never transmit the phrase, "1" followed by "00", as can be deduced in Fig. 3(b). This particular code restriction stabilizes the chaotic saddle whose subshift is generated in Fig. 3(b).

To give some illustrative examples of encoding message in the restricted chaotic signals, say we wish to communicate the following message "BEAT ARMY!" in ASCII format by using the Lorenz attractor:

$$\overbrace{1000010}^{B}\overbrace{1100101}^{E}\overbrace{1100001}^{A}\overbrace{1110100}^{T}\overbrace{0100000}^{\text{space}}\overbrace{1000001}^{A}\overbrace{1110010}^{R}\overbrace{1101101}^{M}\overbrace{1111001}^{Y}\overbrace{0100001}^{!}\,. \tag{16}$$

To transmit the message subject to the "no four zero's in a row" code, a simple way is for the transmitter to insert a buffer bit "$\underline{1}$" after three zeros in a row, regardless of the message bit that follows. Thus, the encoded message becomes,

$$\overbrace{1000\underline{1}010}^{B}\overbrace{1100101}^{E}\overbrace{1100\underline{1}101}^{A}\overbrace{1110100}^{T}\overbrace{0100\underline{1}100}^{\text{space}}\overbrace{1000\underline{1}001}^{A}\overbrace{1110010}^{R}\overbrace{1101101}^{M}\overbrace{1111001}^{Y}\overbrace{0100\underline{1}101}^{!}\,. \tag{17}$$

Furthermore, if the original message contains the block 0001, with three zeros in a row, the modified block is 0001$\underline{1}$1. Thus, the receiver can recover the original message simply by stripping a one after every block of three zeros. Since for the Lorenz attractor, its intrinsic grammar is already included in the rule "no four zeros in a row," the message "BEAT ARMY!" can now be transmitted using the Lorenz circuit [Cuomo & Oppenheim, 1993] by utilizing small control methods outlined in [Hayes *et al.*, 1993]. One may also consider a more severe restriction such as "no three zeros in a row," which corresponds to a larger gap across the partition line. In this case, the encoded binary sequence looks like,

$$\overbrace{100\underline{1}00\underline{1}10}^{B}\overbrace{1100\underline{1}101}^{E}\overbrace{1100\underline{1}0011}^{A}\overbrace{11101001}^{T}\overbrace{0100\underline{1}0010}^{\text{space}}\overbrace{100\underline{1}00\underline{1}01}^{A}\overbrace{11100\underline{1}10}^{R}\overbrace{1101101}^{M}\overbrace{1111001\underline{1}}^{Y}\overbrace{0100\underline{1}0011}^{!}\,. \tag{18}$$

Counting the number of bits in the above three transmissions: the straight ASCII message in Eq. (16) requires 70-bits, the "no 0000" buffered message in Eq. (17) requires 75 bits, and the "no 000" buffered message in Eq. (18) requires 84 bits. Since more buffer bits are needed for more restrictive codes, the transmission rate will be slower, but the code is more immune to noise as the noise-resisting gap is wider.

By over restricting the code, one does not take full advantage of the natural chaotic dynamics produced by the oscillator, resulting in a communication system with reduced transmitter capacity. Dynamically, the transmitter capacity is quantified by the topological entropy of the invariant set in which the message-carrying trajectory lies. The information theory point of view is that topological entropy is the rate at which information is generated when one observes the system. In communication, the topological entropy is the transmitter capacity because this entropy defines the "amount" of information rate that can be be produced [Blahut, 1998]. Thus, in order to optimize the transmitter capacity, one must design a code that maximizes the topological entropy. Since a chaotic saddle is an invariant subset embedded in the original chaotic attractor, the topological entropy of the saddle is generally smaller than that of the attractor. While a larger size of the noise-gap about the partition renders the symbolic dynamics more robust against noise, the resulting chaotic saddle possesses smaller topological entropy. This is due to the fact that widening the noise-gap corresponds to increasing the grammatical restrictions on the permissible codes in the symbol dynamics representation.

The topological entropy of a Markov subshift Σ_2' is equivalent to,

$$h_T(\Sigma_2') = \ln(\rho(A))\,, \tag{19}$$

where A is the transition matrix of its right-resolving presentation (when it exists), and $\rho(A)$ is its spectral radius [Lind & Marcus, 1995; Kitchens, 1998]. Therefore, choosing a large word length, $n = 14$ allows 2^{14} possible permutations of n-bit words, and requires a $2^{14} \times 2^{14}$ transition matrix A. Successively canceling out the corresponding vertices as in Fig. 3(b) is equivalent to zeroing the similarly indexed rows and columns of A. Computing $\ln(\rho(A))$ allows us to produce Fig. 8 showing $h_T(\Sigma_2')$ as a function of gap width ε.

5.2. *The devil's staircase topological entropy versus noise-gap function*

We expect topological entropy to be a monotonically nonincreasing function of k. Increased restrictions on the grammar lead to decreased transmitter capacity. Increasing n, the word size considered, better approximates the effect of continuously increasing the gap size s from $s = 0$; a small increase in s requires n large enough to account for a whole (small) bin which is eliminated. Figure 8 reveals a devil's staircase-like function $h_T(s)$ for $n = 14$. As n is increased, more constant intervals, or "flat spots," are revealed. These flat spots might seem surprising given their origin by the above sequence of spectral-radius calculations; the explanation lies in the fact that invariance of the subshift has required us to eliminate all transitions away from an eliminated node, and often this may effectively eliminate other nearby nodes by cutting-off access to these nodes. In such a case, further widening of the gap, and hence elimination of the next node in the Gray ordering, causes no change because that node may have already been dynamically eliminated in a previous step. The devil's staircase structure arises from the fact that this mechanism occurs on all scales, to 2^n node directed graph representations of the symbol dynamics of the chaotic saddles $M(s)$, for all n, and the larger the n-bit word size first eliminated, the smaller will be the flat spot.

The fact that the topological entropy of the chaotic saddle decreases only slightly in a range of gap sizes $(0, \Delta s)$ has important practical implications. Say the noise amplitude is $\Delta s/10$. Then the chaotic saddles with gap sizes in $(\Delta s/10, \Delta s)$ are immune to noise, yet their transmitter capacity is only slightly less than that of the original chaotic attractor. There are an infinite number of codes that can generate chaotic saddles with gap sizes in $(\Delta s/10, \Delta s)$. From the stand point of transmitter capacity and noise resistance, these codes are therefore optimal. Similar results appear to hold for high-dimensional chaotic systems [Lai & Bollt, 1999].

6. Feedback Control of the Successive Maxima Map

Suppose that we have a chaotic attractor of a flow. The idea of controlling chaos by staying within the chaotic attractor's natural behavior by using only small feedback controls was a natural but brilliant epiphany [Ott *et al.*, 1990], using sensitive dependance to initial condition to our advantage.

Feedback control of a chaotic trajectory may be realized by small parameter variations. For example, given a flow of $x(t) \in \mathbf{R}^N$ where we explicitly write the parameter dependence $p \in \mathbf{R}^n$,

$$\dot{x} = F(x, p)\,, \tag{20}$$

(take the Lorenz equations for example, Eq. (1)), one can hope to affect the trajectory in a predictable manner in the short run. In particular, if the desired short-term response is small, a Lipschitz continuous right-hand side F provides that small parameter variations should suffice. Furthermore for small enough desired short term responses, the required parameter variation can be usefully and easily found by directly solving a two-point-boundary-value-problem (TPBVP). More specifically, suppose that on the surface of section M, the initial condition $x_0 \in M$ flows forward under Eq. (20) to $x_1 \in M$, $x_0 = f(x_0) = \Phi_t(x_0)$ (t is the time of flight of the mapping, which is generally not uniform with respect to x, and this is not a concern to us here) at next Poincaré surface piercing, under a nominal/uncontrolled parameter value p_0. The Poincaré mapping we now denote,

$$f(x, p) : M \to M\,, \tag{21}$$

to emphasize a family of mappings parameterized by accessible parameter p. If we prefer the next iterate to be x_{desired}, then the next controlled response, is a solution to the equation,

$$x_{\text{desired}} = f(x_0, p_1) \tag{22}$$

whose solution is formally a TPBVP of the flow Eq. (20), where p_1 is the unknown in the equation to be found, usually by shooting [Press *et al.*, 1988]. For long duration of flight, the general TPBVP is expected to be numerically unreasonable to solve. However, since we assume $\|x_{\text{desired}} - x_0\|_2 < \varepsilon$ for a small $\varepsilon > 0$, and continuity of the flow with respect to parameter and spacial variations, we expect that $\|p_1 - p_0\|_2$ will be likewise small. In such a case, a standard shooting algorithm, based on Newton's method generally works well [Bollt, 2001], choosing $p = p_0$ as the initial seed. A solution exists for small enough $\varepsilon > 0$, and nonsingular Jacobian derivative, by continuation of the trivial solution $x_1 = f(x_0, p_0)$ along a parameterized solution manifold, $\delta p(x)$, and $x = f(x_0, p_0 + \delta p(x))$, which is

an application of the implicit function theorem. In fact, the linearized equations of variation, $\delta\dot{x} = (\partial F/\partial x)(x, p) \cdot \delta x + (\partial F/\partial p)(x, p) \cdot \delta p$, can often be used to directly solve for p_1, to good approximation, where $\partial F/\partial x$ and $\partial F/\partial p$ are respectively the Jacobian matrices of x and p variations. This generalizes the main idea behind the special case of the OGY technique [Ott *et al.*, 1990], in which $x_{\rm desired}$ is chosen to lie on the stable manifold of an unstable periodic point. The pole-placement version of OGY was written about in a general higher dimensional form in [Romerias *et al.*, 1992]. Note that parametric control works particularly well when controlling unstable periodic orbits since the required parametric variations quickly become negligible.

A significant technical difficulty to our purposes is that once the parameters have been varied, even slightly to say $p_0 + \delta p$, the flow is pushed away from the nominal attractor of p_0. If the perturbation is small, and the negative Lyapunov exponents of the nominal p_0 attractor are large, then the expectation is that the trajectory will quickly settle back towards the nominal attractor, once the parameter is returned to its nominal value of p_0. On the other hand, if the parameters were left at the new perturbed values $p_0 + \delta p$, then the flow could settle to a new and slightly deformed version of the attractor. However, for our purposes of pushing an arbitrary bit into the shift registrar during each successive iteration of the map, parametric variations must be applied at each step. Hence, while our parameter variations are expected to remain small, they are not expected to become negligible as in OGY. Therefore we must correct the map-based prediction of linear response.

We discuss below a black-box approach, whereby all of the necessary temporal and parametric variation responses can be learned from an experiment running on the fly, such as was introduced in [Dolnik & Bollt, 1998].

In particular, we describe here the parametric feedback rules for the successive maxima map as if the flow behaved as a truly one-dimensional map. Then we make corrections to allow for the fact that we vary the parameters at each step, therefore never allowing the response trajectory to settle back to the attractor. Suppose we have an interval map, $f_p : [a, b] \to [a, b]$ such as approximately given by the Lorenz successive maxima map, Eq. (2) and fixed parameter values (say the nominal parameter value is $p_0 = (10, 28, 8/3)$). Suppose $f_{p_0}(x)$ shifts a 0 into the corresponding bit registrar, but we need a 1 (or vice-versa). For example, suppose $\sigma(x) = 0.010101\ldots$ to 7-bit precision, and suppose that $s(\sigma(x)) = \sigma(f_{p_0}(x)) = 0.1010100\ldots$, but we prefer $\sigma(f_p(x)) = 0.1010101\ldots$. Then by continuity of the homeomorphism Eq. (8) and the metric in the symbol space Eq. (7), only a small temporal variation is needed — the more bits used for the register, the smaller the temporal variation. Let

$$\Delta f(x) = f_{\rm des}(x) - f(x)\,, \tag{23}$$

which is small, for any controlled iteration $x = x_n$, where $f(x)$ is the uncontrolled response, and $f_{\rm des}(x)$ puts the required bit in the bit registrar. The map-based analysis performed in [Bollt & Dolnik, 1997; Bollt, 1997] follows the linearization of f with respect to p,

$$\Delta f(x) \approx \left.\frac{\partial f_p^1}{\partial p}\right|_{(p_0,x)} \delta p, \quad \text{or } \delta p \approx \frac{\Delta f(x)}{\left.\dfrac{\partial f_p^1}{\partial p}\right|_{(p_0,x)}}\,. \tag{24}$$

The partial derivatives $\partial f^1/\partial p$ represent the "dynamic shift" of the one-dimensional map due to parameter variations. Because the full dynamics occurs as a flow of the differential equations, a small parameter variation does not generally occur as predicted by the one-dimensional map representation on the surface of section. The dynamic shift defines the *observed* iterative variation of the map immediately after the control parameter is varied.

The fact that an arbitrary message requires controlling parameter perturbations during every iteration is an important technical issue which prevents us from returning to the nominal parameter value p_0. Instead, the $(n+1)$th "uncontrolled" iteration of x assumes that the parameter from nth iteration p_n is unchanged. Therefore, instead of the nominal 1-D map $f_{p_0}(x)$, the estimate of $f(x)$ in Eq. (23) uses the map $f_{p_n}(x)$ which corresponds to the parameter p_n,

$$f(x) = f_{p_n}(x_n)\,. \tag{25}$$

We estimate $f_{p_n}(x_n)$ by linearization around the nominal map $f_{p_0}(x)$:

$$f_{p_n}(x_n) = f_{p_0}(x_n) + (p_n - p_0)\left.\frac{\partial f}{\partial p}\right|_{(x_n,p_0)}\,. \tag{26}$$

Combining Eqs. (23)–(26) we obtain the required

parameter perturbation δk_{n+1}.

$$\delta p_{n+1} = p_{n+1} - p_n = \frac{f_{\text{des}}(x_n) - f_{p_0}(x_n) - (p_n - p_0)\left.\frac{\partial f}{\partial p}\right|_{(x_n,p_0)}}{\left.\frac{\partial f^1}{\partial p}\right|_{(x_n,p_0)}}. \tag{27}$$

The derivative $\partial f/\partial p$ characterizes the rate of the static map variations. To estimate this quantity, one must experimentally "iterate" the one-dimensional maps obtained for several successive Poincaré sections, for three values of the *fixed* adjustable parameter p. Each time a simulation with a new value of p is started, the first intersection with Poincaré surface is neglected, because it is not part of static 1-D map. In our previous chemical reaction application [Dolnik & Bollt, 1998], we have dealt with unavoidable noise fluctuations, by application of cubic smoothing spline fits [Hutchinson, 1986]. We estimate the derivatives $\partial f/\partial p$ from the equation,

$$\left.\frac{\partial f}{\partial p}\right|_{(x,p_0)} = \frac{f_{p+\varepsilon}(x) - f_{p_0}(x)}{\varepsilon}. \tag{28}$$

Direct application of the above formulas would require random access to initial conditions, which is generally not possible in learning the real physical experiment. We proposed a method [Dolnik & Bollt, 1998] of learning these quantities on-the-fly by appropriate manipulations of a running experiment. The dynamic rate of map variations, $\partial f^1/\partial p$, can be learned experimentally. As described in figures in more detail in [Dolnik & Bollt, 1998], we wait for two iterates at the nominal value p_0, between experimental parameter variations, to make sure that the transients settle onto the 1-D attractor, to a high degree of accuracy. The observed next piercing of the Poincaré surface, after a parameter variation, is the dynamic response $f^1(x)$. Each two-iterate-time interval of fixed $p(t) = p_0$ are followed by a one "iterate" time interval of $p(t) = p_0 \pm \varepsilon$. The response function $x(t)$ must be read accordingly. After sampling this dynamic response value $f^1(x)$, we reset the flow rate back to the nominal value for two reference events. This procedure can be repeated, or a perturbation with the same amplitude but of opposite sign can be applied. By periodically repeating this process with positive and negative perturbations, we learn dynamic responses $f^1_{p_0\pm\varepsilon}(x)$ for values of x ergodically scattered throughout the

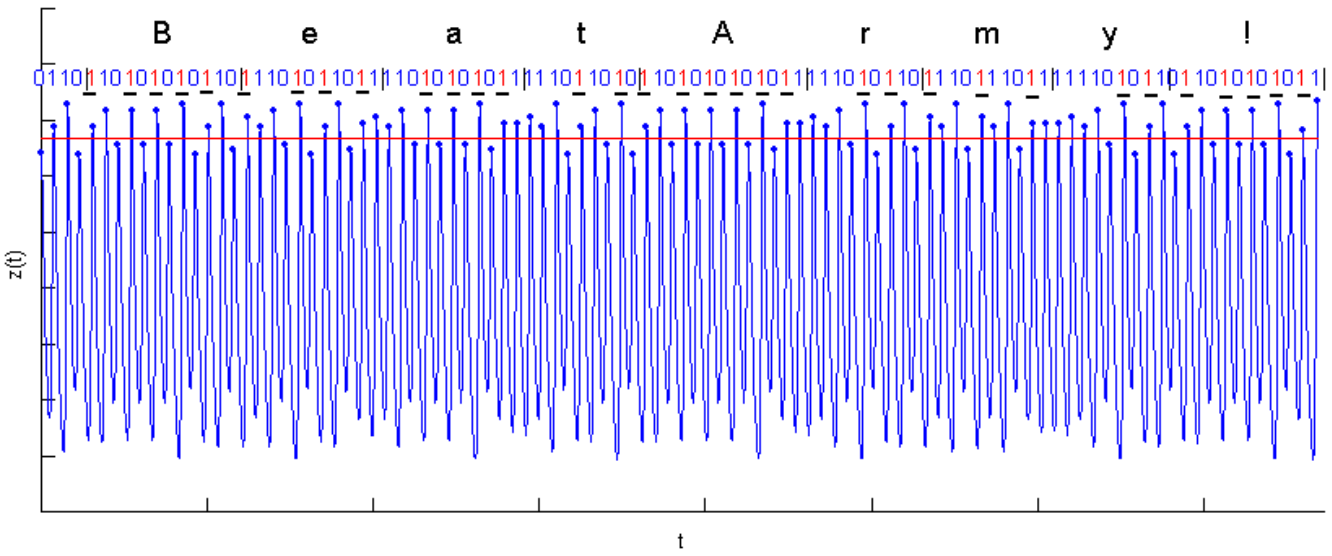

Fig. 9. The $z(t)$ time-series from the Lorenz Equations, Eqs. (1), can be controlled to any desired message, when successive maxima are read relative to the generating partition, which is the horizontal line. This particular $z(t)$ time-series is from the $(x(t), y(t), z(t))$ trajectory shown in Fig. 1. The underlined bits denote noninformation bearing buffer bits which are necessary either due to nonmaximal topological entropy of the underlying attractor, or further code restrictions which were added for noise resistance, as discussed in Sec. 5. The code used was the "no-two zero's in a row" rule, which requires a buffer "1"-bit be inserted after every "0"-bit appears. The message is encoded in standard ASCII, and requires 63-bits, but with the extra 33 buffer bits, the total transmission is slowed to 96-bits. This particularly restrictive code has a topological entropy of $h_T = \ln((1+\sqrt{5})/2) \approx 0.4812$, but gives a particularly wide noise gap.

interval. The derivative $\partial f^1/\partial p$ is estimated similarly to the derivative $\partial f/\partial p$, from the difference quotient:

$$\left.\frac{\partial f^1}{\partial p}\right|_{(x,p_0)} = \frac{f^1_{p_0+\varepsilon}(x) - f_{p_0}(x)}{\varepsilon}\,. \qquad (29)$$

More details are given in [Dolnik & Bollt, 1998] concerning these necessary technical considerations to control a one-dimensional map derived by successive maxima of a measured time-series of a differential equation, or real experiment. We conclude this section by presenting for the first time a plot in Fig. 9 of a controlled trajectory of the Lorenz equations which have been forced to follow a path whose $z(t)$ time-series corresponds to a popular message at the author's home institution.

Acknowledgments

The author was supported by the NSF under Grant No. DMS-9704639 during 1997–2000, and currently under No. DMS-0071314. I would like to thank, Ying-Cheng Lai, Milos Dolnik, Celso Grebogi, Karol Życzkowski, Ted Stanford, Ruslan Davidchack, Mukesh Dhamala, Eric Kostelich, Jim Meiss and Aaron Klebanoff, with whom I have had the pleasure to work on research in the areas of communication with chaos, or symbolic dynamics, or control of chaos, and some of this research is reviewed here.

References

Afraimovich, V. S., Verichev, N. N. & Rabinovich, M. I. [1986] "Stochastic synchronization of oscillations in dissipative systems," *Inv. VUZ Rasiofiz. RPQAEC* **29**, 795–803.

Alvarez, E., Fernandez, A., Garcia, P., Jimenez, J. & Marcano, A. [1999] "New approach to chaotic encryption," *Phys. Lett.* **A263**, p. 373.

Blahut, R. E. [1988] *Principles and Practice of Information Theory* (Addison-Wesley, NY).

Bollt, E. [1997] "Controlling the chaotic logistic map," *PRIMUS* **VII**(1), 1–18.

Bollt, E. & Dolnik, M. [1997] "Encoding information in chemical chaos by controlling symbolic dynamics," *Phys. Rev.* **E55**(6), 6404–6413.

Bollt, E., Lai, Y. C. & Grebogi, C. [1997] "Analysis of the topological entropy versus noise resistance tradeoff when communicating with chaos," *Phys. Rev. Lett.* **79**(19), 3787–3790.

Bollt, E. & Lai, Y. C. [1998] "Dynamics of coding in communicating with chaos," *Phys. Rev.* **E58**(2), 1724–1736.

Bollt, E., Stanford, T., Lai, Y.-C. & Zyczkowski, K. [2000] "Validity of threshold-crossing analysis of symbolic dynamics from chaotic time series," *Phys. Rev. Lett.* **85**(16), 3524–3527.

Bollt, E. [2001] "Combinatorial control of global dynamics in a chaotic differential equation," *Int. J. Bifurcation and Chaos* **11**(8), 2145–2162.

Bollt, E., Stanford, T., Lai, Y.-C. & Zyczkowski, K. [2001] "What symbolic dynamics do we get with a misplaced partition? On the validity of threshold crossings analysis of chaotic time-series," *Physica* **D154**(3&4), 259–286.

Boulant, G., Bielawski, S., Derozier, D. & Lefranc, M. [1997a] "Experimental observation of a chaotic attractor with a reverse horseshoe topological structure," *Phys. Rev.* **E55**, R3801–R3804.

Boulant, G., Lefranc, M., Bielawski, S. & Derozier, D. [1997b] "Horseshoe templates with global torsion in a driven laser," *Phys. Rev.* **E55**, 5082–5091.

Bowen, R. [1970] "Markov partitions for axiom A diffeomorphisms," *Am. J. Math.* **92**, 725–747.

Bowen, R. [1975a] *Equilibrium States and the Ergodic Theory of Anosov Diffeomorphisms* (Springer-Verlag, Berlin).

Bowen, R. [1975b] *Equilibrium States and the Ergodic Theory of Anosov Diffeomorphisms* (Springer-Verlag, Berlin).

Christiansen, F. & Politi, A. [1996] "Symbolic encoding in symplectic maps," *Nonlinearity* **9**, 1623–1640.

Christiansen, F. & Politi, A. [1997] "Guidlines for the construction of a generating partition in the standard map," *Physica* **D109**, 32–41.

Cuomo, K. & Oppenheim, A. V. [1993] "Circuit implementation of synchronized chaos with applications to communications," *Phys. Rev. Lett.* **71**, 65–68.

Cvitanovic, P. [1988] "Invariant measurements of strange sets in terms of cycles," *Phys. Rev. Lett.* **61**, 2729–2732.

Cvitanovic, P., Gunaratne, G. & Procaccia, I. [1988] "Topological and metric properties of Hénon-type attractors," *Phys. Rev.* **A38**, 1503–1520.

Cvitanovic, P. [1991] "Periodic orbits as the skeleton of classical and quantum chaos," *Physica* **D51**, p. 138.

Cvitanovic, P. [1995] "Dynamical averaging in terms of periodic orbits," *Physica* **D83**, 109–123.

Davidchack, R. L. & Lai, Y.-C. [1999] "Efficient algorithm for detecting unstable periodic orbits in chaotic systems," *Phys. Rev.* **E60**, 6172–6175.

Davidchack, R., Lai, Y.-C., Bollt, E. & Dhamala, M. [2000] "Estimating generating partitions of chaotic systems by unstable periodic orbits," *Phys. Rev.* **E61**(2), 1353–1356.

Daw, C. S., Kennel, M. B., Finney, C. E. A. & Connolly, F. T. [1998] "Observing and modeling nonlinear

dynamics in an internal combustion engine," *Phys. Rev.* **E57**, 2811–2819.

de Melo, W. & van Strein, S. [1992] *One-Dimensional Dynamics* (Springer-Verlag, NY).

Devaney, R. L. [1989] *An Introduction to Chaotic Dynamical Systems*, 2nd edition (Addison Wesley, Redwood City, CA).

Diakonos, F. K., Schmelcher, P. & Biham, O. [1998] "Systematic computation of the least unstable periodic orbits in chaotic attractors," *Phys. Rev. Lett.* **81**(20), 4349–4352.

Dolnik, M. & Bollt, E. [1998] "Communication with chemical chaos in the presence of noise," *Chaos* **8**(3), 702–710.

Engbert, R., Scheffczyk, C., Krampe, R., Kurths, J. & Kliegl, R. [1998] *Nonlinear Time Series Analysis of Physiological Data* (Springer-Verlag, Heidelbert), pp. 271–282.

Forney, G. D., Jr. [1974] "Convolutional codes II: Maximum-likelihood decoding," *Inform. Contr.* **25**, 222–226.

Galias, Z. [1999] "Proving the existence of periodic solutions using global interval Newton method," *Proc. IEEE Int. Symp. Circuits and Systems*, ISCAS'99, Vol. VI, Orlando, pp. 294–297.

Galias, Z. [2001] "Interval methods for rigorous investigations of periodic orbits," *Int. J. Bifurcation and Chaos* **11**(9), 2427–2450.

Galias, Z. [2002] "Proving the existence of long periodic orbits in 1D maps using Newton method and backward shooting," *Topol. Its Appl.* **124**(1), 25–37.

Grassberger, P., Kantz, H. & Moenig, U. [1989] "On the symbolic dynamics of the Hénon map," *J. Phys.* **A22**, 5217–5230.

Hansen, K. [1992] "Pruning of orbits in four-disk and hyperbola billiards," *Chaos* **2**, 71–75.

Hansen, K. [1993] "Symbolic dynamics. I. Finite dispersive billiards," *Nonlinearity* **6**, 753–769.

Hayes, S., Grebogi, C. & Ott, E. [1993] "Communicating with chaos," *Phys. Rev. Lett.* **70**, 3031–3034.

Hayes, S., Grebogi, C., Ott, E. & Mark, A. [1994] "Experimental control of chaos for communication," *Phys. Rev. Lett.* **73**, 1781–1784.

Heller, J. A. & Jacobs, I. M. [1971] "Viterbi decoding for satellite and space communications," *IEEE Trans. Commun. Technol.* **COM-19**, 835–848.

Huebner, U., Abraham, N. B. & Weiss, C. O. [1989] "Dimensions and entropies of chaotic intensity pulsations in a single-mode far-infrared NH3 laser," *Phys. Rev.* **A40**, 6354–6365.

Hutchinson, M. F. [1986] "ALGORITHM 642: A fast procedure for calculating minimum cross-validation cubic smoothing splines," *ACM Trans. Math. Software* **12**, 150–153.

Kennedy, M. P. & Kolumbán, G. [2000] "Digital communications using chaos," *Sign. Process.* **80**(7), 1307–1320.

Kitchens, B. P. [1998] *Symbolic Dynamics, One-sided, Two-sided and Countable State Markov Shifts* (Springer, NY).

Kolumbán, G., Kis, G. Jákó, Z. & Kennedy, M. P. [1998] "FM-DCSK: A robust modulation scheme for chaotic communications," *IEICE Trans. Fundam. Electron., Commun. Comput. Sci.* **E81-A**(9), 1798–1802.

Kolumbán, G. & Kennedy, M. P. [2000] "Overview of digital communications," in *Application of Chaotic Electronics to Telecommunications*, eds. Kennedy, M. P., Rovatti, R. & Setti, G. (CRC Press, FL), pp. 131–149.

Kurths, J., Voss, A., Saparin, P., Witt, A., Kleiner, H. J. & Wessel, N. [1995] "Quantitative analysis of heart rate variability," *Chaos* **5**, 88–94.

Lai, Y.-C., Bollt, E. & Grebogi, C. [1999] "Communicating with chaos using high-dimensional symbolic dynamics," *Phys. Lett.* **A255**(1&2), 75–81.

Lefranc, M., Glorieux, P., Papoff, F., Molesti, F. & Arimondo, E. [1994] "Combining topological analysis and symbolic dynamics to describe a strange attractor and its crises," *Phys. Rev. Lett.* **73**, 1364–1367.

Lehrman, M. & Rechester, A. B. [1997] "Extracting symbolic cycles from turbulent fluctuation data," *Phys. Rev. Lett.* **78**, 1–4.

Lin, S. & Costello, D. J. [1982] *Error Control Coding* (Prentice Hall, Englewood Cliffs, NJ).

Lind, D. & Marcus, B. [1995] *An Introduction to Symbolic Dynamics and Coding* (Cambridge University Press, NY).

Lorenz, E. N. [1963] "Deterministic nonperiodic flow," *J. Atmos. Sci.* **20**, 130–141.

Michelson, A. M. & Levesque, A. H. [1985] *Error Control Techniques for Digital Communication* (John Wiley, NY).

Milnor, J. & Thurston, W. [1997] *On Iterated Maps of the Interval I and II* (Princeton University Press, Princeton).

Mischaikow, K., Mrozek, M., Reiss, J. & Szymczak, A. [1999] "Construction of symbolic dynamics from experimental time series," *Phys. Rev. Lett.* **82**, 1144–1147.

Ott, E., Grebogi, C. & Yorke, J. A. [1990] "Controlling chaos," *Phys. Rev. Lett.* **64**, 1196–1199.

Pecora, L. M. & Carroll, T. L. [1990] "Synchronization in chaotic systems," *Phys. Rev. Lett.* **64**, p. 821.

Pecora, L. M., Carroll, T. L., Johnson, G. A. & Mar, D. J. [1997] "Fundamentals of synchronization in chaotic systems, concepts, and applications," *Chaos* **7**, 520–543.

Peterson, W. W. & Weldon, E. J., Jr. [1972] *Error Correcting Codes*, 2nd edition (The MIT Press, Cambridge, MA).

Pless, V. [1998] *Introduction to the Theory of Error-Correcting Codes*, 3rd edition (John Wiley, NY).

Press, W., Flannery, B., Teukolsky S. & Vetterling, W. [1988] *Numerical Recipes in C, The Art of Scientific Computing* (Cambridge University Press, NY).

Robinson, C. [1995] *Dynamical Systems: Stability, Symbol Dynamics, and Chaos* (CRC Press, Ann Arbor).

Romerias, F., Grebogi, C., Ott, E. & Dayawansa, W. [1992] "Controlling chaotic dynamical systems," *Physica* **D58**(1002), 165–192.

Rudolph, D. J. [1990] *Fundamentals of Measurable Dynamics, Ergodic Theory on Lebesgue Spaces* (Clarendon Press, Oxford).

Schmelcher, P. & Diakonos, F. K. [1997] "Detecting unstable periodic orbits of chaotic dynamical systems," *Phy. Rev. Lett.* **78**(25), 4733–4736.

Schmelcher, P. & Diakonos, F. K. [1998] "General approach to the localization of unstable periodic orbits in chaotic dynamical systems," *Phys. Rev.* **E57**(3), 2739–2746.

Schweizer, J. & Schimming, T. [2001a] "Symbolic dynamics for processing chaotic signals-I: Noise reduction of chaotic sequences," *IEEE Trans. Circuits Syst.* **48**(11), 1269–1282.

Schweizer, J. & Schimming, T. [2001b] "Symbolic dynamics for processing chaotic signals-II: Communication and coding," *IEEE Trans. Circuits Syst.* **48**(11), 1283–1294.

Smale, S. [1967] "Differentiable dynamical systems," *Bull AMS* **73**, p. 747.

Yamada, T. & Fujisaka, H. [1983] "Stability theory of synchronized motion in coupled-oscillator systems. II," *Progr. Theor. Phys.* **70**, p. 1240.

Yamada, T. & Fujisaka, H. [1984] "Stability theory of synchronized motion in coupled-oscillator systems. III," *Progr. Theor. Phys.* **72**, p. 885.